Out-of-Bounds Hydrodynamics in Anisotropic Dirac Fluids

Julia M. Link, Boris N. Narozhny, Egor I. Kiselev, and Jörg Schmalian

Phys. Rev. Lett. **120**, 196801 — Published 10 May 2018

DOI: 10.1103/PhysRevLett.120.196801

Out-of-bounds hydrodynamics in anisotropic Dirac fluids

Julia M. Link,[1] Boris N. Narozhny,[1,2] Egor I. Kiselev,[1] and Jörg Schmalian[1,3]

[1] *Institute for Theory of Condensed Matter, Karlsruhe Institute of Technology (KIT), 76131 Karlsruhe, Germany*
[2] *National Research Nuclear University MEPhI (Moscow Engineering Physics Institute), 115409 Moscow, Russia*
[3] *Institute for Solid State Physics, Karlsruhe Institute of Technology (KIT), 76131 Karlsruhe, Germany*

(Dated: April 9, 2018)

We study hydrodynamic transport in two-dimensional, interacting electronic systems with merging Dirac points at charge neutrality. The dispersion along one crystallographic direction is Dirac-like, while it is Newtonian-like in the orthogonal direction. As a result, the electrical conductivity is metallic in one and insulating in the other direction. The shear viscosity tensor contains six independent components, which can be probed by measuring an anisotropic thermal flow. One of the viscosity components vanishes at zero temperature leading to a generalization of the previously conjectured lower bound for the shear viscosity to entropy density ratio.

Hydrodynamic flow in quantum many-body systems is essential in systems as diverse as superfluid Helium [1], (Al,Ga)As heterostructures [2], cold atomic "gases" [3–5], and the quark-gluon plasma [5, 6]. Recently, it has become possible to study in greater detail the hydrodynamic flow of electrons [7, 8] via transport measurements in graphene, yielding a breakdown of the Wiedemann-Franz law [9], super-ballistic transport [10, 11], negative local resistance [12, 13], and giant magnetodrag [14] (for a recent review see Ref. 15 and 16). Other key examples are ultra-pure $PdCoO_2$ [17] and Weyl semimetals [18]. The appeal of these experiments is that they allow for an investigation of the universal collision-dominated dynamics of the pure electron fluid, largely independent of its couplings to the lattice and impurities: the hydrodynamic flow is expected when electron-electron scattering dominates over impurity and electron-phonon scattering processes [15].

Hydrodynamics is also one of the most successful applications of the duality between strongly coupled gauge theories and gravity theory [19], leading to the lower bound [20] for the ratio of the shear viscosity and entropy density

$$\eta/s \geqslant \hbar/(4\pi k_{\mathrm{B}})\,. \tag{1}$$

While originally derived as an equality for a specific strongly-coupled field theory, the bound was conjectured to apply to all single-component non-relativistic fluids [20]. Thus, to identify a scenario where Eq. (1) is explicitly violated is of fundamental importance. It is also of practical relevance as a small viscosity implies a strong tendency towards turbulent flow [21]. Eq. (1) can already be rationalized using Boltzmann transport theory: Let $s \approx k_{\mathrm{B}}\lambda^{-d}$ be the entropy density (in d dimensions) in terms of the thermal de Broglie wave length λ and $\eta \approx \epsilon\tau\lambda^{-d}$ the shear viscosity with energy density ϵ and scattering time τ. A quasiparticle description of transport suggests that $\epsilon\tau \geqslant \hbar$, leading to the above bound (up to numerical coefficients of order unity). A more formal reasoning can be made using scaling arguments. We rescale distances according to $\boldsymbol{x} \to \boldsymbol{x}' = \boldsymbol{x}/b$ with the scaling factor b. Momentum conservation and hyperscaling for critical systems imply that both the viscosity and entropy density change according to $\eta\,(T) = b^{-d}\eta\,(b^z T)$ and $s\,(T) = b^{-d}s\,(b^z T)$, with the dynamic scaling exponent z. Thus, the entropy density and shear viscosity have the same scaling dimension. If the system approaches a fixed point, the ratio η/s should approach a universal value in units of $\hbar/k_B$. This is analogous to the electrical conductivity in $d = 2$ that approaches a universal value in units of $e^2/\hbar$, a result that follows from $\sigma\,(T) = b^{2-d}\sigma\,(b^z T)$.

The bound (1) appears to be violated in gravity theories dual to an anisotropic version of a super-Yang-Mills plasma [22–24] with applications to cold gases [25]. It is of great interest to identify a solid-state system where such a violation might occur.

In this Letter, we analyze the hydrodynamic behavior in an anisotropic Dirac system, where two Dirac cones merge in momentum space [26]. Such a model is relevant to the organic conductor α-(BEDT-TTF)$_2$I$_3$ under pressure [27] and the heterostructure of the 5/3 TiO_2/VO_2 supercell [28, 29]. Similar behavior is expected in the surface modes of topological crystalline insulators with unpinned surface Dirac cones [30] and quadratic double Weyl fermions [31]. In the collision-dominated regime at charge neutrality, we predict extremely anisotropic electrical transport exhibiting either insulating or metallic behavior depending on the orientation of the applied electric field relative to the crystallographic axes. Similarly, the electronic shear viscosity strongly depends on the flow direction, exhibiting fundamentally different temperature behavior. As a result, at low temperatures the viscosity to entropy density ratio may diverge, stay constant, or vanish, depending on the spatial direction. In the latter case, the Eq. (1) is violated, an effect with experimentally measurable consequences through viscous thermal Hagen–Poiseuille flow. We explain the anisotropic transport in terms of the emergence of multiple length scales. In addition we propose a generalization of the viscosity bound to two-dimensional anisotropic sys-

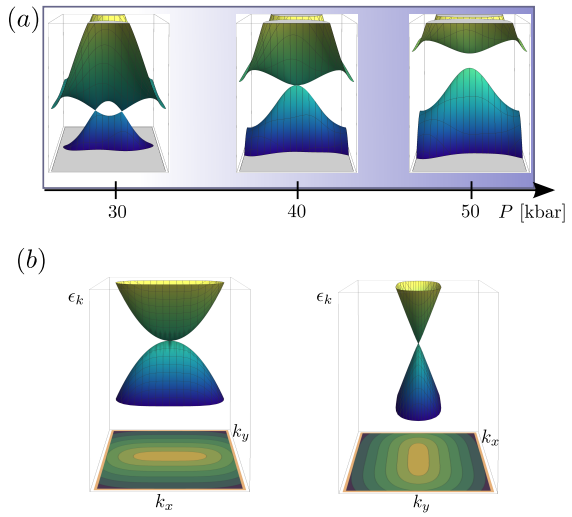

FIG. 1. Upper panel (a): merging Dirac cones of the organic conductor α-(BEDT-TTF)$_2$I$_3$ under the application of the uniaxial pressure [27]. At $P_a = 40$ kbar, the two Dirac cones merge resulting in an anisotropic dispersion. Lower panel (b): energy dispersion of the Hamiltonian (3).

tems:

$$\frac{\eta_{\alpha\beta\alpha\beta}}{s} \geqslant \frac{1}{4\pi}\frac{\hbar}{k_B}\frac{\sigma_\alpha}{\sigma_\beta}, \qquad \frac{\eta_{\alpha\beta\beta\alpha}}{s} \geqslant \frac{1}{4\pi}\frac{\hbar}{k_B}, \tag{2}$$

which includes the electrical conductivity anisotropy as an additional observable. The numerical coefficient $1/4\pi$ is consistent with Ref. 23.

The model. Anisotropic Dirac systems are described by the model Hamiltonian, $H = H_0 + H_C$, where the single-particle part is

$$H_0 = \int d^2r\, \psi_r^\dagger \left(-\frac{1}{2m}\nabla_x^2\sigma_x - iv\nabla_y\sigma_y\right)\psi_r, \tag{3}$$

and H_C is the electron-electron Coulomb interaction with two-body potential $V(r-r') = e^2/|r-r'|$. Here, v is the velocity along the y-direction and the Pauli matrices $\sigma_{x,y}$ describe the pseudo-spin space. The dispersion in the x-direction is characterized by the mass m or, alternatively, by the momentum scale $k_0 = mv$. The anisotropy in Eq. (3) is enforced by the underlying lattice. Specifically, the direction of the parabolic dispersion (the x-direction) is along the axis of the two merging Dirac points, see Fig. 1. In the organic conductor α-(BEDT-TTF)$_2$I$_3$ [27], the two Dirac cones merge together upon applying uniaxial pressure. According to Ref. 27, an anisotropic Dirac cone is expected to form at $P = 40$ kbar, see Fig. 1. From Ref. 32, it follows that the dimensionless strength of the Coulomb interaction is of order unity, which is important to reach a sufficiently wide temperature regime where electron-electron scattering dominates.

The renormalization group behavior of this model was recently investigated in Ref. [26] within a large-N expansion [33, 34] (N is the number of fermion flavors; $N=2$ for the organic charge transfer salts and $N=8$ for the oxide interfaces). While an analysis is possible for arbitrary values of the coupling constant $\alpha = e^2/(\hbar v)$, we focus here on the strong coupling behavior. In this regime, the flow equations are [26]:

$$\frac{d\alpha}{d\log b} = -\frac{0.362}{N}\alpha, \qquad \frac{dk_0}{d\log b} = \frac{0.2374}{N}k_0. \tag{4}$$

This gives rise to two characteristic length scales

$$\lambda_x \propto T^{-\phi/z}, \qquad \lambda_y \propto T^{-1/z}, \tag{5}$$

with the dynamic scaling exponent, $z = 1-0.362/N$. The additional crossover exponent $\phi = (1-0.2374/N)/2$ is a measure of the anisotropy. $z < 1$ reflects an increase of the velocity at low energies and $\phi < 1/2$ implies that interactions make the anisotropy even stronger if compared to the bare spectrum of Eq.(3). The fact that $\phi \neq 1$ is the most crucial ingredient of our subsequent discussion. The violation of the lower bound only requires $\phi \neq 1$ as one viscosity component vanishes faster than s for $T \to 0$ even if the large-N approach turns out to be quantitatively inaccurate.

Scaling. Now we consider the constitutive relations in anisotropic systems. The electrical conductivity is a rank-two tensor defined in the standard way, $j_\alpha = \sigma_{\alpha\beta}E_\beta$ (with $\alpha, \beta \in \{x, y\}$). The viscosity is a rank-four tensor connecting the dissipative part of the stress tensor $\tau_{\alpha\beta}$ and the flow velocity gradient, $\tau_{\alpha\beta} = \sum_{\gamma\delta}\eta_{\alpha\beta\gamma\delta}\partial_\gamma u_\delta$. The number of independent conductivity and viscosity coefficients can be found from symmetry arguments [35]. In a rotationally invariant system, both the conductivity and shear viscosity are each characterized by a single independent coefficient: $\sigma_{\alpha\beta} = \sigma\delta_{\alpha\beta}$ and $\eta_{\alpha\beta\gamma\delta} = \eta\left(\delta_{\alpha\gamma}\delta_{\beta\delta} + \delta_{\alpha\delta}\delta_{\beta\gamma} - \delta_{\alpha\beta}\delta_{\gamma\delta}\right)$ [35]. In this Letter, we focus on incompressible fluids and hence do not consider the bulk viscosity. In contrast, the Hamiltonian (3) is not rotationally invariant and is characterized by two conductivity elements σ_{xx} and σ_{yy} and six independent viscosity coefficients with $\eta_{\alpha\beta\gamma\delta} = \eta_{\gamma\delta\alpha\beta}$, such that

$$\begin{pmatrix}\tau_{xx}\\ \tau_{xy}\\ \tau_{yx}\\ \tau_{yy}\end{pmatrix} = \begin{pmatrix}\eta_{xxxx} & 0 & 0 & \eta_{xxyy}\\ 0 & \eta_{xyyx} & \eta_{xyxy} & 0\\ 0 & \eta_{yxyx} & \eta_{yxxy} & 0\\ \eta_{yyxx} & 0 & 0 & \eta_{yyyy}\end{pmatrix}\begin{pmatrix}\partial_x u_x\\ \partial_y u_x\\ \partial_x u_y\\ \partial_y u_y\end{pmatrix}. \tag{6}$$

Below we show that the "off-diagonal" momentum relaxation along the y-direction (with linear dispersion) due to a flow with velocity along the x-direction (of parabolic dispersion) described by η_{xyxy} is clearly different from the "opposite" case, η_{yxyx}.

The scaling behavior of the conductivity and the viscosity follows from the Kubo formalism [36, 37]. If one takes charge conservation into account, the scaling dimension of the conductivity is a purely "geometric" effect that involves the length scales λ_α. If b is a scaling parameter for length scales along the y-direction, it follows

[26, 38]

$$\sigma_{xx}(T) = b^{\phi-1}\sigma_{xx}(b^z T),$$
$$\sigma_{yy}(T) = b^{1-\phi}\sigma_{yy}(b^z T). \quad (7)$$

Fixing the coefficient b via $b^z T = const$ reveals that b is given by the ratio of the two length scales $b^{\phi-1} \to \lambda_x/\lambda_y$. It immediately follows that $\sigma_{yy} \propto T^{(\phi-1)/z}$ diverges as $T \to 0$, while $\sigma_{xx} \propto T^{(1-\phi)/z}$ vanishes. The system is insulating along the direction with parabolic dispersion and metallic in the other direction. Below, we confirm this behavior within an explicit kinetic theory and see that this behavior is pronounced below the characteristic temperature $k_B T_0 \equiv mv^2 \approx 1.5$ eV in the organic salts.

Similar behavior emerges for the entropy density and the components of the viscosity tensor. For the entropy density, it follows from the usual scaling behavior of anisotropic systems [39], $s(T) = b^{-(1+\phi)}s(b^z T)$, yielding $s(T) \propto k_B/(\lambda_x\lambda_y)$. To determine the behavior of the viscosity tensor we use again the Kubo formalism (the details are summarized in the supplementary material [40]). The result is that most tensor elements $\eta_{\alpha\beta\gamma\delta}$ have the same scaling dimension as $s(T)$. However, there are two crucial exceptions:

$$\eta_{xyxy}(T) = b^{-(3-\phi)}\eta_{xyxy}(b^z T),$$
$$\eta_{yxyx}(T) = b^{-(3\phi-1)}\eta_{xyxy}(b^z T). \quad (8)$$

It immediately follows that $\eta_{xyxy}/s \propto T^{2(1-\phi)/z}$ and $\eta_{yxyx}/s \propto T^{-2(1-\phi)/z}$. Unless the system is isotropic and $\phi = 1$, one component vanishes and the other diverges. Thus, regardless of the numerical coefficient of η_{xyxy}, it will violate the bound Eq. (1) at sufficiently low temperatures since $\phi < 1$. Below we obtain this behavior from Boltzmann theory as well. The scaling analysis reveals that the charge transport and momentum transport are closely related to each other. This allows us to construct combinations of physical observables that have scaling dimension zero. These combinations are listed in Eq. (2) and give rise to the generalized lower bound for the viscosity tensor.

Hydrodynamics. The scaling behavior can be obtained from the kinetic equation

$$\frac{\partial f_{\mu\boldsymbol{k}}}{\partial t} + \boldsymbol{v}_{\mu\boldsymbol{k}} \cdot \frac{\partial f_{\mu\boldsymbol{k}}}{\partial \boldsymbol{x}} + e\boldsymbol{E} \cdot \frac{\partial f_{\mu\boldsymbol{k}}}{\partial \boldsymbol{k}} = I^{ee}_{\mu}, \quad (9)$$

where $f_{\mu\boldsymbol{k}}$ is the distribution function for a quasiparticle from the band μ and with the quasi-momentum $\boldsymbol{k}$, and I^{ee}_{μ} is the collision integral due to the Coulomb interaction. The latter we treat in perturbation theory in $1/N$ (for details see Refs. 40 and 41).

Following the standard derivation of the hydrodynamic theory in the limit of an incompressible fluid [21], we integrate the kinetic equation (9) and obtain generalizations of the Navier-Stokes equation at the charge neutrality point. Flow along the direction of the parabolic dispersion is described by a Navier-Stokes equation similar to

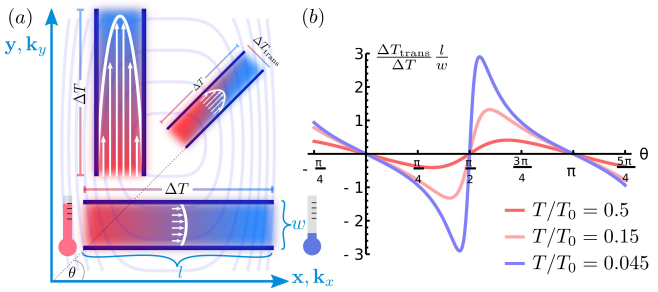

FIG. 2. Left panel: Hagen-Poiseuille flow profile due to a temperature gradient. The bound-violating small ratio η_{xyxy}/s leads to a parabolic flow profile with large curvature and yields a large thermal conductivity, while the large ratio η_{yxyx}/s yields almost ohmic flow (b): Transverse temperature gradient as function of the angle θ between flow direction and x-axes (see left panel).

that of a Galilean invariant system,

$$m_* n(\partial_t u_x + u_i\partial_i u_x) + \partial_x P = \mathcal{F}_{s,x} + m_* n\partial_i \delta j^i_I, \quad (10)$$

where $m_* \approx 1.37m$, n is the total quasiparticle density, $\delta\boldsymbol{j}_I$ is the dissipative correction to the total quasiparticle current, P is the hydrodynamic pressure, and $\mathcal{F}_{s,\beta} = \partial_\alpha \tau_{\alpha\beta} = \partial_\alpha \eta_{\alpha\beta\gamma\delta}\partial_\gamma u_\delta$ is the Stokes force. Flow in the y-direction obeys the equation similar to that in graphene [42, 43]

$$Ts(\partial_t u_y + u_i\partial_i u_y) + \partial_y P + u_y\partial_t P = \quad (11)$$
$$= \mathcal{F}_{s,y} - u_y E_i \delta j_i + u_y \partial_{x_i}\delta j_{\epsilon,i}.$$

The dissipative terms include the corrections to the electric current, $\delta\boldsymbol{j}$, and the energy current, $\delta\boldsymbol{j}_\epsilon$.

The simplest nontrivial solution of these equations can be obtained in the linearized stationary regime in the absence of the electric field. Using Eq. 6, we find

$$\partial_\alpha P = \tilde{\eta}_{\alpha\alpha\alpha\alpha}\partial^2_\alpha u_\alpha + 2\tilde{\eta}_{\alpha\alpha\overline{\alpha}\overline{\alpha}}\partial_\alpha\partial_{\overline{\alpha}} u_{\overline{\alpha}} + \tilde{\eta}_{\overline{\alpha}\alpha\overline{\alpha}\alpha}\partial^2_{\overline{\alpha}} u_\alpha \quad (12)$$

with $\tilde{\eta}_{\alpha\beta\gamma\delta} = \frac{1}{2}(\eta_{\alpha\beta\gamma\delta} + \eta_{\gamma\beta\alpha\delta})$, and $\overline{x} = y$ and vice versa. Note that $\tilde{\eta}_{xyxy} = \eta_{xyxy}$ and same for $\tilde{\eta}_{yxyx}$. From the kinetic equation it also follows that the heat current, $\boldsymbol{j}_\epsilon \approx (5/3)\epsilon\boldsymbol{u}$, is solely determined by the flow velocity. This is similar to the particle current in Galilean-invariant systems and reflects the fact that the thermal conductivity of a Dirac system at neutrality is infinite in the limit of infinite size [44, 45]. Using $\partial_\alpha P = -s\partial_\alpha T$ at neutrality, we can solve the above equations for a finite geometry, find the velocity profile $\boldsymbol{u}$, and determine the thermal current from $\boldsymbol{j}_\epsilon$. Note that this is how the entropy density enters our theory.

Consider now a flow in a system of width w. In this geometry, there is no net flow in the lateral x-direction. The solution of Eq. (12) with the no-slip boundary conditions, $u_y(x = \pm w/2) = 0$, yields the standard Hagen-Poiseuille profile

$$u_y(x) = \frac{s}{2\eta_{xyxy}}\left(\frac{w^2}{4} - x^2\right)\partial_y T. \quad (13)$$

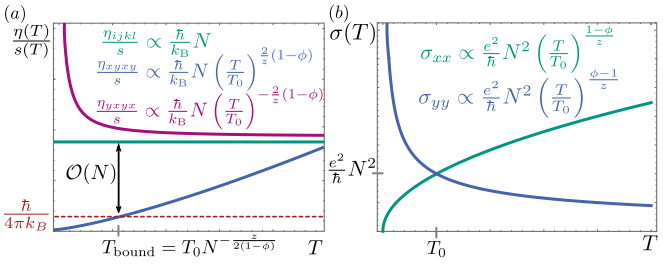

FIG. 3. Upper panel (a): the ratio $\eta_{\alpha\beta\gamma\delta}/s$ as a function of temperature. The viscosity coefficient η_{xyxy} violates the lower bound (shown by the dashed line). Lower panel (b): $\sigma_{\alpha\alpha}$ as function of temperature with insulating and metallic conductivity along the direction with parabolic and linear dispersion, respectively.

Integration over the cross section yields the total thermal current $I_\epsilon = w\kappa_{yy}\partial_y T$ with the thermal conductivity $\kappa_{yy} = (5\epsilon w^2/24)(s/\eta_{xyxy})$. Similar analysis of the flow along the x-direction yields $\kappa_{xx} = (5\epsilon w^2/24)(s/\eta_{yxyx})$. In the case of no-stress boundary conditions it is better to analyze conical flow.

The above results demonstrate that the thermal Hagen–Poiseuille flow is determined precisely by those viscosity tensor elements (8) that violate the ordinary scaling behavior. Thus, the ratios η_{xyxy}/s and η_{yxyx}/s matter and are in fact the easiest to observe. The other tensor components emerge only when the flow direction is not aligned with one of the crystalline axes. In this case a transverse temperature gradient builds up, see Fig. 2.

Kinetic theory. Finally, we use the microscopic quantum kinetic equation approach to find the conductivities and viscosities. The former can be found in the standard way [21]: applying a weak electric field, $\boldsymbol{E}$, we drive the system out of equilibrium where the distribution function $f_{\mu\boldsymbol{k}}$ acquires a nonequilibrium correction proportional to the field: $\delta f_{\mu\boldsymbol{k}} = f^{(0)}_{\mu\boldsymbol{k}}(1-f^{(0)}_{\mu\boldsymbol{k}})h_{\mu\boldsymbol{k}}/T$, $h_{\mu\boldsymbol{k}} = \mu \boldsymbol{v}_{\mu\boldsymbol{k}} \boldsymbol{E} g^{\boldsymbol{E}}_{\mu\boldsymbol{k}}$. Solving the kinetic equation for the functions $g^{\boldsymbol{E}}_{\mu\boldsymbol{k}}$, we find $\sigma_{xx,yy}(T) \propto N^2(e^2/\hbar)(T/T_0)^{\pm(1-\phi)/z}$ in agreement with the scaling results.

To determine the viscosity, we have to find the stress tensor within linear response to the external shear force. In terms of the nonequilibrium distribution function, the stress tensor is given by $\tau_{\alpha\beta} = \sum_\mu \int_k v^\alpha_{\mu\boldsymbol{k}} k_\beta \delta f_{\mu\boldsymbol{k}}$. The correction $\delta f_{\mu\boldsymbol{k}}$ is proportional to the velocity gradients with $h_{\mu\boldsymbol{k}} = \sum_{\alpha\beta} \mu (v^\alpha_{\mu\boldsymbol{k}} k_\beta - \delta_{\alpha\beta}\epsilon_{\mu\boldsymbol{k}}/2)\partial_\alpha u_\beta g^\beta_{\mu\boldsymbol{k}}$. Now we expand the functions $g^\beta_{\mu\boldsymbol{k}}$ in the basis of the eigenfunctions of the linearized kinetic equation [43, 46], $g^\beta_{\mu\boldsymbol{k}} = \sum_n \psi^\beta_n \phi^{(n)}_{\mu\boldsymbol{k}}$. The dominant contribution comes from the two modes describing the energy and the energy band index. This allows us to represent the kinetic equation (9) in the matrix form, $\mathcal{M}^{ee}_{u_{\beta,\alpha}} \boldsymbol{\psi}^\beta = \boldsymbol{G}_{u_{\beta,\alpha}}$, where the matrix $\mathcal{M}^{ee}_{u_{\beta,\alpha}}$ corresponds to the collision integral due to Coulomb interaction. The exact form of $\mathcal{M}^{ee}_{u_{\beta,\alpha}}$ and $\boldsymbol{G}_{u_{\beta,\alpha}}$ can be found in Ref. 40. Solving the matrix equation, we find $g^\beta_{\mu\boldsymbol{k}}$ and hence the viscosity coefficients, $\eta_{\alpha\beta\gamma\delta} = \sum_\mu \int_k \mu v^\alpha_{\mu\boldsymbol{k}} k_\beta (v^\gamma_{\mu\boldsymbol{k}} k_\delta - \delta_{\gamma\delta}\epsilon_{\mu\boldsymbol{k}}/2) g^\beta_{\mu\boldsymbol{k}} f^{(0)}_{\mu\boldsymbol{k}}(1-f^{(0)}_{\mu\boldsymbol{k}})/T$. At charge neutrality, the resulting viscosities are given by $\eta_{\alpha\beta\gamma\delta} = N^2 \mathcal{C}_{\alpha\beta\gamma\delta}(k_0^2/\hbar)(T/T_0)^{\phi_{\alpha\beta\gamma\delta}}$, where $\mathcal{C}_{\alpha\beta\gamma\delta}$ are numerical coefficients of order unity. The exponents $\phi_{\alpha\beta\gamma\delta}$ coinside with the results of the above scaling analysis.

The linear-response solution of the quantum kinetic equation yields the entropy density in the scaling form, $s = N\mathcal{C}_s k_B (k_0^2/\hbar^2)(T/T_0)^{(1+\phi)/z}$. Due to the linear dispersion in the y-direction, the velocity component v_y at the scale T is larger than v_x. The viscosity coefficient η_{yxyx} describes the flow of the momentum k_x with the larger velocity component v_y leading to the diverging ratio η_{yxyx}/s. In contrast, the viscosity coefficient η_{xyxy} corresponds to the flow of the momentum k_y with the much slower velocity v_x, leading to the violation of the bound. The ratios of the viscosity coefficients to the entropy density are shown in Fig. 3.

Summary. In this letter, we have shown that anisotropic Dirac systems are fascinating new materials with unparalleled transport properties in the hydrodynamic regime. The same material exhibits both insulating and metallic behavior depending on the direction of the applied electrical field. Furthermore, the shear viscosity is represented by a fourth rank tensor with six independent components with the ratio $\eta_{\alpha\beta\gamma\delta}/s$ that may either vanish or diverge, see Fig. 3. In the former case, the universal bound (1) appears to be violated. We demonstrated that these viscosity tensor elements can be measured via viscous thermal flow, where the more electrically conducting direction is also the direction of larger thermal conductivity. The thermal flow in the direction with the linear spectrum is expected to be highly susceptible to turbulence and should lead to large transverse temperature variations. (see right panel of Fig.2). Similar behavior will also occur in other anisotropic systems, such as critical bosonic systems at a Lifshitz point [39]. The ratio η/s (1) was introduced to have a measure for the strength of interaction in a quantum fluid. Our analysis shows that the violation of the bound for anisotropic systems is not necessarily an indicator for extreme interactions, but reflects the fact that η/s is no longer an appropriate measure of the interaction strength in anisotropic systems. We have suggested a generalization of the lower bound that takes into account the anisotropy. The generalized bound (2) offers a better quantification of fluid interactions. Nevertheless, the smallness of the viscosity to entropy density ratio $\eta/s \ll \hbar/(4\pi k_B)$ for anisotropic systems remains a strong indicator for a tendency towards turbulent flow.

We gratefully acknowledge illuminating discussions with A. V. Chubukov, I. V. Gornyi, K. Kanoda, J. Klier, A. D. Mirlin, M. Müller, D. E. Sheehy, and T. Neupert. J.M.L. thanks the Carl-Zeiss-Stiftung for finan-

cial support. B.N.N. acknowledges support by the EU Network Grant FP7-PEOPLE-2013-IRSES 612624 "InterNoM" and the MEPhI Academic Excellence Project (Contract No. 02.a03.21.0005). The work of J.S. was performed in part at the Aspen Center for Physics, which is supported by NSF grant PHY-1607611.

¿

[1] D. Vollhardt and P. Wölfle, *The Superfluid Phases of Helium 3* (Taylor & Francis Ltd, 1990).

[2] M. J. M. de Jong and L. W. Molenkamp, Phys. Rev. B **51**, 13389 (1995).

[3] C. Chafin and T. Schäfer, Phys. Rev. A **87**, 023629 (2013).

[4] T. Enss, R. Haussmann, and W. Zwerger, Ann. Phys. (Amsterdam) **326**, 770 (2011).

[5] T. Schäfer, Annu. Rev. Nucl. Part. Sci. **64**, 124 (2014).

[6] E. Shuryak, Prog. Part. Nucl. Phys. **53**, 273 (2004).

[7] R. N. Gurzhi, Zh. Eksp. Teor. Fiz. **44**, 771 (1963), [Sov. Phys. JETP 17, 521 (1963)].

[8] R. N. Gurzhi, Usp. Fiz. Nauk **94**, 689 (1968), [Sov. Phys. Usp. 11, 255 (1968)].

[9] J. Crossno, J. K. Shi, K. Wang, X. Liu, A. Harzheim, A. Lucas, S. Sachdev, P. Kim, T. Taniguchi, K. Watanabe, T. A. Ohki, and K. C. Fong, Science **351**, 1058 (2016).

[10] H. Guo, E. Ilseven, G. Falkovich, and L. S. Levitov, PNAS **114**, 3068 (2017).

[11] R. Krishna Kumar, D. A. Bandurin, F. M. D. Pellegrino, Y. Cao, A. Principi, H. Guo, G. H. Auton, M. B. Shalom, L. A. Ponomarenko, G. Falkovich, I. V. Grigorieva, L. S. Levitov, M. Polini, and A. K. Geim, Nature Physics **13**, 1182 (2017).

[12] D. A. Bandurin, I. Torre, R. Krishna Kumar, M. Ben Shalom, A. Tomadin, A. Principi, G. H. Auton, E. Khestanova1, K. S. Novoselov, I. V. Grigorieva1, L. A. Ponomarenko, A. K. Geim, and M. Polini, Science **351**, 1055 (2016).

[13] L. S. Levitov and G. Falkovich, Nature Phys. **12**, 672 (2016).

[14] M. Titov, R. V. Gorbachev, B. N. Narozhny, T. Tudorovskiy, M. Schütt, P. M. Ostrovsky, I. V. Gornyi, A. D. Mirlin, M. I. Katsnelson, K. S. Novoselov, A. K. Geim, and L. A. Ponomarenko, Phys. Rev. Lett. **111**, 166601 (2013).

[15] B. N. Narozhny, I. V. Gornyi, A. D. Mirlin, and J. Schmalian, Annalen der Physik **529**, 1700043 (2017).

[16] A. Lucas and K. C. Fong, Journal of Physics: Condensed Matter **30**, 053001 (2018).

[17] P. J. W. Moll, P. Kushwaha, N. Nandi, B. Schmidt, and A. P. Mackenzie, Science **351**, 1061 (2016).

[18] J. Gooth, F. Menges, C. Shekhar, V. Süß, N. Kumar, Y. Sun, U. Drechsler, R. Zierold, C. Felser, and B. Gotsmann, (2017), arXiv:1706.05925.

[19] J. M. Maldacena, Adv. Theor. Math. Phys. **2**, 231 (1998).

[20] P. K. Kovtun, D. T. Son, and A. O. Starinets, Phys. Rev. Lett. **94**, 111601 (2005).

[21] E. M. Lifshitz and L. P. Pitaevskii, *Physical Kinetics* (Pergamon Press (Oxford), 1981).

[22] A. Rebhan and D. Steineder, Phys. Rev. Lett. **108**, 021601 (2012).

[23] S. Jain, R. Samanta, and S. P. Trivedi, Journal of High Energy Physics **2015**, 28 (2015).

[24] S. Cremonini, Mod. Phys. Lett. B **25**, 1867 (2011).

[25] R. Samanta, R. Sharma, and S. P. Trivedi, (2016), arXiv:1607.04799.

[26] H. Isobe, B.-J. Yang, A. Chubukov, J. Schmalian, and N. Nagaosa, Phys. Rev. Lett. **116**, 076803 (2016).

[27] A. Kobayashi, Y. Suzumura, F. Piéchon, and G. Montambaux, Phys. Rev. B **84**, 075450 (2011).

[28] V. Pardo and W. E. Pickett, Phys. Rev. Lett. **102**, 166803 (2009).

[29] S. Banerjee, R. R. P. Singh, V. Pardo, and W. E. Pickett, Phys. Rev. Lett. **103**, 016402 (2009).

[30] C. Fang and L. Fu, Phys. Rev. B **91**, 161105 (2015).

[31] S.-M. Huang, S.-Y. Xu, I. Belopolski, C.-C. Lee, G. Chang, T.-R. Chang, B. Wang, N. Alidoust, G. Bian, M. Neupane, D. Sanchez, H. Zheng, H.-T. Jeng, A. Bansil, T. Neupert, H. Lin, and M. Z. Hasan, PNAS **113**, 1180 (2016).

[32] M. Hirata, K. Ishikawa, K. Miyagawa, M. Tamura, C. Berthier, D. Basko, A. Kobayashi, G. Matsuno, and K. Kanoda, Nature Communications **7**, 12666 (2016).

[33] M. S. Foster and I. L. Aleiner, Phys. Rev. B **77**, 195413 (2008).

[34] D. T. Son, Phys. Rev. B **75**, 235423 (2007).

[35] L. D. Landau and E. M. Lifshitz, *Fluid mechanics*, 2nd ed. (Butterworth-Heinemann, Oxford, 1998).

[36] B. Bradlyn, M. Goldstein, and N. Read, Phys. Rev. B **86**, 245309 (2012).

[37] A. Principi, G. Vignale, M. Carrega, and M. Polini, Phys. Rev. B **93**, 125410 (2016).

[38] D. E. Sheehy and J. Schmalian, Phys. Rev. Lett. **99**, 226803 (2007).

[39] R. M. Hornreich, M. Luban, and S. Shtrikman, Phys. Rev. Lett. **35**, 1678 (1975).

[40] See Supplemetal Material at ... for details of the calculations, which includes Refs. [26,35,36].

[41] M. Schütt, P. M. Ostrovsky, I. V. Gornyi, and A. D. Mirlin, Phys. Rev. B **83**, 155441 (2011).

[42] M. Müller, J. Schmalian, and L. Fritz, Phys. Rev. Lett. **103**, 025301 (2009).

[43] U. Briskot, M. Schütt, I. V. Gornyi, M. Titov, B. N. Narozhny, and A. D. Mirlin, Phys. Rev. B **92**, 115426 (2015).

[44] M. Müller, L. Fritz, and S. Sachdev, Phys. Rev. B **78**, 115406 (2008).

[45] M. S. Foster and I. L. Aleiner, Phys. Rev. B **79**, 085415 (2009).

[46] B. N. Narozhny, I. V. Gornyi, M. Titov, M. Schütt, and A. D. Mirlin, Phys. Rev. B **91**, 035414 (2015).